OXFORD
SOT | Society of Toxicology
academic.oup.com/toxsci
Tox Spotlight article

Toxicological Sciences, 2026, **209(4)**, kfag035
https://doi.org/10.1093/toxsci/kfag035
Advance Access Publication Date: March 21, 2026
Research Article

Temporal variation in markers of immune signaling and wound repair in primary human airway epithelial cells following acute versus repeated woodsmoke condensate exposure

Elise Hickman [1,2,3], Chloe K. Chou [1,2], Cole Seifert [2], Jessie Chappel [1,2], Yong Ho Kim [4], Elizabeth Corteselli [1,3], Julia E. Rager [1,2,3,*]

[1]Curriculum in Toxicology and Environmental Medicine, School of Medicine, University of North Carolina-Chapel Hill, Chapel Hill, NC 27599, United States
[2]Department of Environmental Sciences and Engineering, Gillings School of Global Public Health, University of North Carolina-Chapel Hill, Chapel Hill, NC 27599, United States
[3]Center for Environmental Medicine, Asthma, and Lung Biology, School of Medicine, University of North Carolina-Chapel Hill, Chapel Hill, NC 27599, United States
[4]Center for Public Health and Environmental Assessment, United States Environmental Protection Agency, Research Triangle Park, NC 27711, United States

*Corresponding author: Department of Environmental Sciences and Engineering, The University of North Carolina at Chapel Hill, 135 Dauer Drive CB 7431, Chapel Hill, NC 27599, United States. Email: jrager@unc.edu.

Abstract

Wildfire smoke (WFS) exposures are becoming more common, and firefighters and community members are often exposed to WFS for days to weeks. Controlled studies assessing the effects of repeated exposure to WFS and woodsmoke (WS; as a surrogate for WFS) or compared acute versus repeated exposure have evaluated a limited number of timepoints and endpoints using rodent models. Here, we leveraged differentiated primary human bronchial epithelial cells (HBECs) to test the hypothesis that different molecular responses occur upon acute versus repeat exposures to WS. HBECs (n = 4 donors) were exposed to 22 μg/cm^2 red oak WS condensate for an acute, 4-h exposure, or repeat exposures of 4 h/d, 3 d/wk, across 2 wk. Membrane permeability, cell viability, and transcriptional responses were measured at the end of each exposure paradigm, and secreted proteins were measured throughout the repeat exposure. Acute exposure significantly increased expression of genes involved in fibrosis and immune response, whereas repeated exposure significantly decreased expression of genes involved in tissue repair and remodeling. Secreted protein responses were similar to transcriptomic responses and demonstrated temporal variation in response to exposure. This study supports the feasibility of using HBECs to evaluate acute and repeat WS exposures and indicates differential responses from these exposures with direct relevance to pulmonary disease processes, including those involved in fibrosis, asthma, and chronic obstructive pulmonary disease. These findings highlight the need for future studies to better understand molecular responses to repeated smoke exposures.

Keywords: lung cells; interindividual responses; temporal; transcriptomics; proteomics; wildfire

The incidence and severity of wildfire events is growing, resulting in increased exposure to wildfire smoke (WFS) worldwide (Westerling et al. 2006; Hurteau et al. 2014). WFS is a complex and variable chemical mixture that contains hundreds of different chemicals, including gasses, particulate matter, volatile organic compounds, and polycyclic aromatic hydrocarbons (Reisen et al. 2015; Black et al. 2017; Kim et al. 2018; Wentworth et al. 2018; Rice et al. 2023; Zhang et al. 2025a), many of which have been linked to adverse health effects (Kyung and Jeong 2020; Låg et al. 2020; Alford and Kumar 2021; Rizzo and Rizzo 2025). Epidemiological studies show that acute exposure to WFS is associated with respiratory symptoms and increased risk of hospitalizations due to respiratory disease exacerbation and cardiovascular conditions (Delfino et al. 2009; Mirabelli et al. 2009; Reid et al. 2016; Orr et al. 2020; Chen et al. 2021; Zhang et al. 2025b). Prolonged exposure to WFS has been associated with decline in lung function, increase in airway hyperresponsiveness, increase in risk of heart failure, and later-in-life cancer outcomes (Liu et al. 1992; Orr et al. 2020; Korsiak et al. 2022; Hao et al. 2025; VoPham et al. 2025). Mechanisms informing these temporally dependent responses require further elucidation.

Mechanisms underlying outcomes associated with acute exposures have been evaluated through in vivo and in vitro experimentation. For example, controlled exposure studies in humans indicate that exposure to woodsmoke (WS) (as a surrogate for WFS) induces local and systemic inflammation and oxidative stress (Barregard et al. 2008; Ghio et al. 2012; Peters et al. 2018; Burbank et al. 2019; Schwartz et al. 2020) and can impact responses to viral infections (Rebuli et al. 2019). In rodents, acute exposure to WS elicits changes in respiratory function, responses to respiratory bacterial and viral infection, immune cell infiltration and function, and cytokine secretion, with degree and

direction of response dependent on fuel type and exposure paradigm (Migliaccio et al. 2013; Sussan et al. 2014; Kim et al. 2018; Vose et al. 2021). Paralleling in vivo findings, in vitro studies have found that exposure to wildfire-relevant WS induces toxicity, inflammation, and oxidative stress and dampens antiviral and antibacterial responses in airway epithelial cells (Brocke et al. 2022; Upadhyay et al. 2024; Heibati et al. 2025; Noël et al. 2025) and macrophages (Hansson et al. 2023; Bazina et al. 2025).

Although these studies provided important foundational knowledge of the molecular mechanisms impacted by acute exposures, many real-world WFS exposures occur over days to weeks, representing a subchronic exposure that may not be accurately modeled by acute WFS and WS exposures. For example, standard deployment for wildfire firefighters is 14 days, during which firefighters often work for 12 to 16 h and stay in camps in close proximity to the wildfire (Navarro et al. 2022; National Interagency Fire Center 2025), and nearby community members are exposed to WFS plumes, significantly impacting air quality for days-to-weeks (Hao et al. 2025; Schollaert et al. 2025). Furthermore, planned increases in prescribed fires to mitigate wildfire risk could increase subchronic exposure to WFS (Sacks et al. 2025). Although the need for better understanding the effects of long-term, repeated WFS exposure has been recognized (Sacks et al. 2025), controlled toxicology studies modeling these effects are relatively limited. One rodent study found that acute exposure to WS resulted in increased neutrophils in bronchoalveolar lavage fluid, whereas repeated exposure resulted in increased eosinophils, macrophages, and lymphocytes (Sussan et al. 2014). Other rodent studies evaluating the effects of repeated exposure demonstrated decreased lung function and alveolar macrophage efferocytosis, coinciding with differential lung gene expression indicating increased oxidative stress and tissue remodeling (Hargrove et al. 2019; Buford et al. 2024; Cochran et al. 2024), though these studies do not directly compare acute versus repeated exposures. In vitro approaches have been used to assess the effects of repeated exposure to other inhaled toxicants (Braakhuis et al. 2020; Janbazacyabar et al. 2022; Mastalerz et al. 2022; Upadhyay et al. 2022; de Lagarde et al. 2024; Zimmermann et al. 2025), but repeated exposure to WFS-relevant conditions has yet to be evaluated. Furthermore, previous studies often lack the use of fully differentiated airway epithelial cells (at air–liquid interface) and generally measure a limited number of proteins or genes. Therefore, more broadly characterizing RNA and secreted protein changes following acute versus repeated exposure to WFS in vitro represents a significant research gap.

One potential reason for the lack of repeated exposure studies is methodologic limitations. Animals and human in vivo designs often require a significant investment of time and resources, particularly when collecting samples at multiple time points. New approach methodologies (NAMs), which aim to reduce the use of animal testing through in silico and in vitro models, can provide an avenue for experimental designs that include repeated exposures (Zavala et al. 2020). These types of studies are challenging in immortalized cell lines due to their lack of physiological relevance and continuous replication. However, primary human airway basal cells from the small airways, bronchi, and nasal passages can be differentiated at the air–liquid interface (ALI) into physiologically relevant epithelial cultures that contain a variety of cell types (e.g., ciliated cells, secretory cells, basal cells) and which can be maintained and repeatedly sampled for extended periods of time (Fulcher et al. 2005; Fulcher and Randell 2013). Because these cultures are derived from human donors, they also allow for more accurate representation of inter-individual variability than immortalized cell lines. This study set out to implement this NAMs-based approach, leveraging a model of fully differentiated bronchial airway epithelial cells from human donors to characterize the effects of acute (4 h) and repeated (4 h/d, 3 d/wk, 2 wk) exposure to wildfire-relevant WS. We evaluated cell viability, barrier integrity, transcriptomic signatures, and secreted proteins to provide a more holistic view on human airway responses over time and to understand conserved and unique responses to acute versus repeated exposure to WS.

Materials and methods

Experimental methods

Cell culture

Primary human airway basal cells from nonsmoking, healthy lung donors were acquired from the UNC Marsico Lung Institute Tissue Culture and Procurement Core. The basal cells supplied by the core were obtained from the trachea and bronchi of human lungs deemed unsuitable for transplantation as described previously (Fulcher et al. 2005; Fulcher and Randell 2013) and as approved by the UNC Institutional Review Board (No. 03-1396). Passage one basal cells were thawed and seeded onto flasks coated with bovine collagen type I (PureCol, AdvanceBiomatrix 5005). Basal cells were cultured in PneumaCult-Ex Plus media (STEMCELL Technologies 05040) supplemented with hydrocortisone (STEMCELL Technologies No. 07925) and penicillin/streptomycin (Thermo Fisher 15140122). Upon reaching approximately 80% confluency, basal cells were passaged onto 12-well permeable inserts (0.4 μm pore, size-polyethylene terephthalate, CELLTREAT Scientific Products 230621) coated with human collagen type IV (Sigma C-7521) at a density of 200,000 cells per well and expanded in PneumaCult-Ex Plus until confluent. Once basal cells reached confluence on inserts, apical media were removed, and basolateral media were replaced with Pneumacult-ALI media (STEMCELL Technologies 05001) supplemented with hydrocortisone, heparin (STEMCELL Technologies 07980), and penicillin/streptomycin. Basal cells were differentiated into pseudostratified ciliated cultures in Pneumacult-ALI media for 4 wk, with daily media changes for the first week and three times per week media changes for the subsequent weeks. Cultures were washed apically once per week with Hank's balanced salt solution (HBSS) with calcium and magnesium (Thermo Fisher 14025076) to remove secretions. Cultures were maintained for an additional 4 wk after differentiation was achieved prior to experimentation. Primary human bronchial epithelial cell (HBEC) cultures differentiated using this and similar methods have been extensively characterized previously, with studies showing that cultures contain ~7 to 10 different cell types, including ciliated cells, goblet cells, club cells, ionocytes, neuroendocrine cells, and basal cells (Ravindra et al. 2021; Lee et al. 2023; Ramirez-Moral et al. 2024). Cultures from 2 males and 2 females (age-matched, one 21-yr-old donor and one 42-yr-old donor per sex) were used for all following experimentation. For additional demographic information, see Table S1. All cells and cultures were maintained in a humidified incubator at 37°C and 5% CO_2 throughout expansion, differentiation, and experimentation.

Histology

To visually assess culture differentiation, cells were stained with hematoxylin and eosin and Alcian Blue PAS. Cells were prepared for fixation by washing the apical surface with 200 μl of

phosphate-buffered saline (PBS) without calcium and magnesium (Thermo Fisher 14190250) for 20 min at 37°C. Apical PBS and basolateral media were aspirated, and 10% neutral buffered formalin (Millipore Sigma HT501128-4L) was added to the apical (200 µl) and basolateral (1 ml) compartments. Formalin-fixed tissues were processed in a Leica ASP 6025S tissue processer and embedded in paraffin (Leica Paraplast) using a HistoCore Arcadia H. Tissues were then sectioned on a microtome (Leica, RM2255) at 5 µm onto positively charged slides (Fisher Scientific, 12-550-15). Before staining, slides were prebaked at 50 degrees Celsius overnight. AB/PAS stains were performed using the Leica Autostainer XL. The slides were stained with Alcian Blue (Anatech, LTD, 867) for 10 min, immersed in Periodic Acid (Thermo Fisher Scientific, A223-100) for 5 min, rinsed in water, then transferred to Schiff reagent (Fisher Scientific, SS32-500) for 30 min followed by a Sulfurous rinse for 1 min, and finally washed in running tap water for 10 min. After staining, slides were then dehydrated and coverslipped with Cytoseal 60 (Epredia, 83104). Hematoxylin & eosin (H&E) stains were performed using the autostainer XL from Leica Biosystems. The slides were stained with Hematoxylin (Epredia, 7211) for 2 mins and eosin-Y (Epredia, 7111) for 1 min. Clarifier 2 (7402) and Bluing (7111) solutions from Epredia were used to differentiate the reaction. After staining, slides were dehydrated in graded ethanol, ending in xylene, and coverslipped with Cytoseal 60 (Epredia, 83104). Slides were imaged using the Aperio AT2 Digital Pathology Scanner (Leica Biosystems) at 40X magnification.

WS particle condensate generation

WS particle condensate was derived from red oak incinerated at smoldering temperatures (500°C) in a quartz tube furnace, collected via cryogenic traps, concentrated, and resuspended at a concentration of 1 mg/ml in PBS as described previously (Kim et al. 2018). Red oak was used (i) because it is a biomass type commonly burned during wildfire events in the central and southeastern United States, with parts of the southeast considered moderate to high wildfire potential by the US Forest Service (Dillon et al. 2015; Kim et al. 2018; United States Forest Service 2023), and (ii) to enable comparison with previous studies of mice and human participants exposed to smoke from smoldering red oak (Kim et al. 2018; Rebuli et al. 2019; Nalesnik et al. 2026). A smoldering burn temperature was prioritized not only for comparison to previous studies but also because smoldering conditions generally persist longer than flaming conditions (Rein and Huang 2021), making smoldering conditions more relevant to repeat exposure scenarios. The resulting condensate collected from the tube furnace system was frozen at −20°C until experimentation. Immediately prior to dilution and cell treatment, the condensate was vortexed and sonicated for 2 min at 60 Hz in a VWR Symphony Ultrasonic Bath (Model 97044-002).

Cell exposure and sample collection

Smoldering red oak condensate was diluted in Pneumacult-ALI media to a concentration of 98.56 µg/ml and applied apically (to the top of the cultures) in 250 µl total volume, corresponding to a dose of 22 µg/cm^2, similar to previously published studies (Brocke et al. 2022; Vitucci et al. 2025). This dose was previously compared with real-world exposures by Vitucci et al. using air pollution PM ranges experienced by firefighters and community members as input for particle dosimetry modeling. This modeling estimated an in vitro dose of 0.4 µg/cm^2 for community members and 19 µg/cm^2 for firefighters. Thus, our experimental conditions represent a higher exposure most relevant to firefighters or to community members experiencing very high exposure. Pneumacult-ALI media with the same amount of PBS as the diluted condensate was used as the vehicle control. Immediately prior to exposure, cultures were washed apically with 100 µl of warmed HBSS, and basolateral media were replaced. For the acute exposure paradigm, cells were exposed for 4 h, with media and cell collection immediately following exposure. For the repeated exposure paradigm, cells were exposed for 4 h, three times per week (Monday, Wednesday, Friday), for 2 wk. This experimental design was chosen to minimize the stress of apical liquid application on cells typically cultured at the ALI and to maintain cells on a standard feeding/media change schedule (Monday, Wednesday, Friday). Basolateral media were collected before each exposure, representing a collection timeframe of approximately 42 h after the end of the previous exposure, with the exception of day 8, which was collected approximately 66 h after the end of the previous exposure. Notably, all sample collections were within 2 to 3 d to maintain consistency among repeated exposure measures while maintaining study feasibility. After each exposure (4 h), the exposure media were removed, the apical side of the cultures was washed with 100 µl warmed HBSS, the basolateral media were collected (postexposure samples), and the basolateral media were replaced with fresh media. Cells were collected immediately following the 4-h exposure on the last day (day 12). Cells were collected in Qiagen Buffer RLT (Qiagen 79216) with 1% 2-mercaptoethanol (Millipore Sigma M6250), and cell lysates were immediately passed through Qiashredder columns (Qiagen 79656). Media and lysates were stored at −80°C until further experimentation. The exposure and sample collection paradigm is summarized in Fig. 1.

Lactate dehydrogenase assay

To assess cytotoxicity from the single acute exposure, as well as throughout the repeated exposure, lactate dehydrogenase activity (LDH) in the basolateral media was measured using the CyQUANT LDH Cytotoxicity Assay Kit (Thermo Fisher Scientific C20301) per manufacturer's instructions. For a positive control, one well from each donor was lysed via apical addition of 1% triton X-100 in 250 µl and incubation of the well for the same period of time as the experimental treatment (4 h). Absorbance at 490 nm (peak) and 680 nm (background) was measured using a SpectraMax iD5 plate reader (Molecular Devices). Percent cytotoxicity was calculated by dividing background- and blank-corrected absorbance from each sample by the positive control absorbance from the corresponding lysed cells from the same donor and multiplying by 100.

Trans-epithelial electrical resistance

To assess epithelial barrier integrity following repeated exposure to red oak condensate, trans-epithelial electrical resistance (TEER) was measured using an EVOM3 (Epithelial Volt/Ohm Meter) and EndOhm 12 mm cup chamber (World Precision Instruments) as described in detail previously (Mallek and McCullough 2021). Coated inserts without cells were used to obtain blank resistance, which was subtracted from measured resistance. Ω x cm^2 was calculated by multiplying the blank-corrected resistance by the surface area of the insert (1.1 cm^2). TEER was considered a nondestructive assay and was measured just before sample collection described in the previous section.

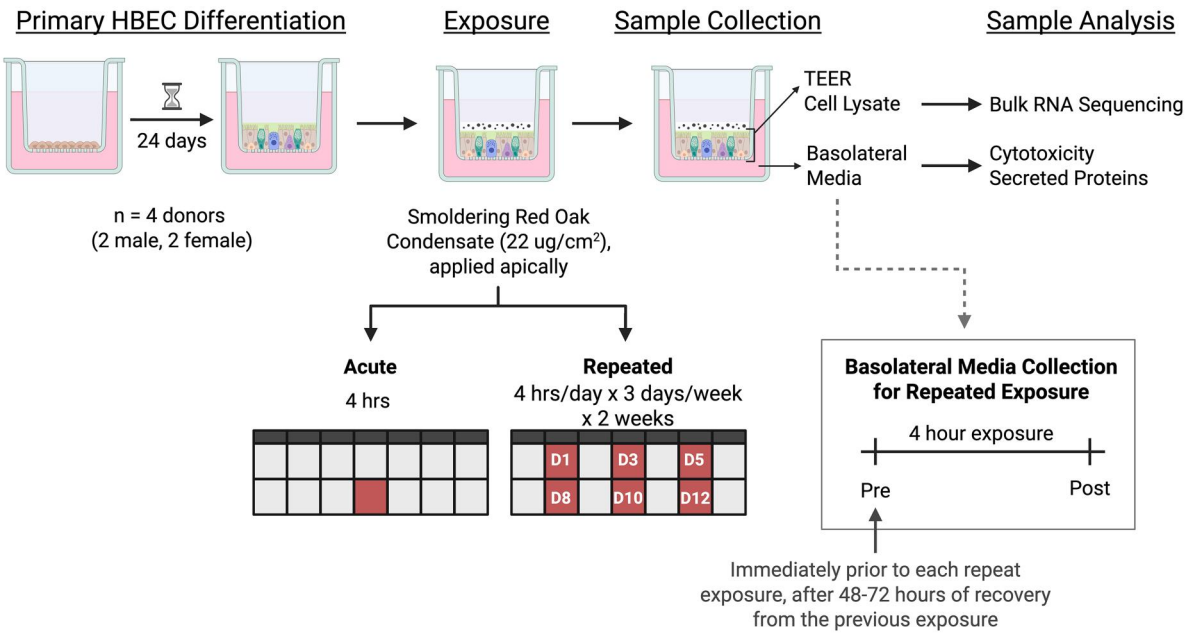

Fig. 1. Schematic of experimental design. Primary human bronchial epithelial cells from four donors were differentiated and exposed apically to 22 μg/cm^2 smoldering red oak condensate. Cells were exposed using either an acute paradigm (4 h) or a repeated paradigm (4 h per day, 3 days per week, for 2 wk). Bulk RNA sequencing was performed on cell lysate collected immediately following the acute exposure and the repeated exposure on day 12. Basolateral media were collected pre- and postexposure each day of the repeated exposure experiment and assayed for secreted proteins and cytotoxicity. Created in BioRender. Hickman, E. (2025) https://BioRender.com/e5cxn4u.

RNA sequencing

RNA was isolated using the Qiagen RNeasy Micro Kit (Qiagen 4004). Concentration and quality were measured using a NanoDrop 100 spectrophotometer (Thermo Fisher). All samples had 260/280 values greater than 2, indicating high quality. RNA libraries for RNA-seq were prepared using the TempO-Seq Assay Kit following manufacturer's protocols and evaluated through the BioSpyder TempO-Seq Human Whole Transcriptome Assay (BioSpyder). Libraries were sequenced with an Illumina NovaSeq X. BioSpyder TempO-Seq R software was used to process the raw data via the following steps: (i) BCL to Fastq (bcl2fastq v2.20.0.422) was used for the base-calling with the use-base mask parameter (Y51, i9, i9 1); (ii) Reads were aligned using STAR aligner (version 2.5.3a) with the end-to-end option, allowing up to two mismatches (genome build: GRCh38/h38); (iii) The count table was generated using featureCounts (version v1.5.3) with default parameters. Further sequencing QA/QC included requiring >6x10^6 mapped reads in positive controls; requiring low signal-to-noise ratios (i.e., total number of mapped reads in positive controls divided by total number of mapped reads in negative controls > 20:1); and requiring >80% of mapped reads in positive controls. All processing steps are available through the Tempo-SeqR pipeline.

Secreted protein measurement

Proteins secreted into the basolateral compartment were measured via the Nomic nELISA MaxPlex and Core Immune assays, which are high-throughput, multiplex assays that combine primary antibody capture with proximity-based colocalization for detection of up to 275 and 283 different proteins, respectively (Tables S2 and S3). Supernatants from treated cells were frozen and sent to Nomic Bio (Montreal, Canada) for Nomic Platform-based secretome analysis using standard protocols, as described previously (Dagher et al. 2025). Briefly, Nomic's nELISA technology pre-assembles antibody pairs on spectrally encoded microparticles, resulting in spatial separation between noncognate antibodies, preventing the rise of reagent-driven cross-reactivity, and enabling multiplexing of hundreds of nELISA assays in parallel. Protein concentrations on microparticles were read out by high-throughput flow cytometry (Bio-Rad ZE5 cell analyzer) and decoded using Nomic's proprietary software. Standard curves for all targets were generated to derive pg/ml values from cytometry fluorescence units.

Data analysis

Reproducibility

Raw and processed RNA sequencing data are available via Gene Expression Omnibus under the accession GSE288818. Raw and processed multi-plex protein expression data are available via the Ragerlab-Dataverse (Hickman et al. 2026). All data were analyzed using R (R Core Team 2025). All associated input files and script are available via the Ragerlab GitHub (2026). Packages used throughout the analysis, in addition to those in base R, included janitor (Firke 2024), openxlsx (Schauberger and Walker 2025), tidyverse (Wickham et al. 2019), patchwork (Pedersen 2025), ggpubr (Kassambara 2025), rstatix (Kassambara 2023), pheatmap (Kolde 2025), and factoextra (Kassambara and Mundt 2020). Additional packages used for specific analyses are detailed below.

LDH and TEER

LDH and TEER data were assessed for normality quantitatively using the Shapiro–Wilk test and qualitatively using histograms and Q–Q plots. Significant differences in cytotoxicity between vehicle and treated cells for the single acute exposure and each day of the repeated exposure were determined using a Wilcoxon signed rank test. Significant differences in TEER between vehicle and treated cells on day 12 of the repeated exposure were determined using a paired t-test.

RNA sequencing

RNA sequencing counts were first evaluated for potential unwanted variation in the data through RUV surrogate variable derivation (Risso et al. 2014), and minimal changes in data distributions were observed; therefore, analyses continued without additional data normalization. Potential sample outliers were assessed via principal component analysis and hierarchical clustering, with no outliers (greater than 6 standard deviations from the mean) detected (Fig. S1). Differential gene expression was assessed using DESeq2 (Love et al. 2014) with the design formula ~ Donor + Exposure_Paradigm. Contrasts were extracted for differences between acute exposure and its vehicle control and between repeated exposure and its day-matched vehicle control. Genes were considered significantly differentially expressed with adjusted P-value < 0.05 and absolute value of the $\log_2$ fold change > 0.585. Overlap in differentially expressed genes between the acute and repeated exposure paradigms was visualized using Euler plots (Larsson 2024). Pathway analysis was conducted with Ingenuity Pathway Analysis (IPA) software (QIAGEN 2025) using P-values and $\log_2$ fold changes for significantly differentially expressed genes. For pathway enrichment statistics, a Benjamini–Hochberg adjusted P-value < 0.05 was considered significant; for activation/inhibition statistics, a z-score > 2 was considered predicted activation, whereas a z-score < -2 was considered predicted inhibition (QIAGEN 2025).

Secreted proteins

Secreted protein data processing and analysis were conducted separately for pre- and post-exposure samples due to differing lengths of cell incubation time with the media (48 to 72 h for pre-samples and 4 h for post-samples). A schematic of the data processing workflow is shown in Fig. S2. Proteins were retained in the dataset if they were detected in at least two donors on at least 1 d in at least one exposure group (vehicle or red oak). Tables S2 and S3 include the upper and lower limit of detections for each protein and whether they were retained in the dataset. Missing values were imputed using GSimp (Wei et al. 2018), an algorithm that allows for imputation above or below a specified limit of detection for each protein. Data from the MaxPlex and CoreImmune panels were then merged. In the case of duplicated proteins between the two panels, data from the CoreImmune panel were retained due to higher sensitivity of that panel. This resulted in 210 proteins in the pre-exposure dataset and 181 proteins in the postexposure dataset. Potential sample outliers were assessed via principal component analysis, with no outliers (greater than 6 standard deviations from the mean) detected (Fig. S3). Data were assessed for normality quantitatively using the Shapiro–Wilk test and qualitatively using histograms and Q–Q plots, and data were $\log_2$ transformed prior to statistical analysis. Paired t-tests within each day were used to assess significant differences in secreted protein concentration between vehicle and red oak-treated cells, with $P < 0.05$ considered significant. To assess overall structural variation between pre- and postexposure proteomic profiles, PERMDISP, a multivariate dispersion test, was implemented using vegan (Oksanen et al. 2025) to evaluate differences in sample spread within each condition. To further account for potential donor-specific effects on overall variability, a linear mixed-effects model was fitted using lme4 (Bates et al. 2015) to per-sample mean pairwise Euclidean distances, with donor included as a random effect and condition and timepoint as fixed effects. Results were visualized using heatmaps and UpSet plots (Lex et al. 2014; Krassowski 2020).

Integration of RNA sequencing and secreted protein data

To understand whether there were correlations between specific gene-to-protein expression levels, and whether there were similar trends following exposure, secreted protein data from day 1 post-exposure and day 3 pre-exposure were compared with the acute exposure RNA sequencing data (day 1 postexposure), and secreted protein data from day 12 postexposure were compared with the repeated exposure RNA sequencing data (day 12 postexposure). The biomaRt (Durinck et al. 2005, 2009) and geneSynonym (Mancarci 2025) packages were used to convert secreted protein Uniprot IDs to gene names and to search the RNA sequencing datasets for gene synonyms in cases of multiple gene names. Spearman correlations were used to understand the relationship between $\log_2$ protein concentration and RNA-sequencing raw counts, with $P < 0.05$ and $|R| > 0.6$ considered significantly correlated. We also compared lists of significantly differentially expressed genes and proteins to determine overlap in significance and directionality of change following red oak exposure between the endpoints.

Results

Confirmation of culture integrity

Primary HBEC culture differentiation was confirmed prior to experimentation using Alcian Blue PAS staining for mucins and hematoxylin and eosin staining for general histology (Fig. S4). Smoldering red oak condensate exposure did not elicit significant changes in cell viability or TEER in comparison with vehicle exposure (Fig. S5).

RNA sequencing differential expression

To characterize transcriptomic responses to smoldering red oak and determine whether responses differ between acute (4 h) and repeated (4 h/d, 3 d/wk, 2 wk) exposure conditions, bulk RNA sequencing was performed. Cellular RNA samples were specifically collected immediately following the 4-h acute exposure and immediately following the 4-h exposure on day 12 of the repeated exposure paradigm. For all genes that were measured in this analysis, alongside their full gene names, see Table S4. A total of 214 genes were differentially expressed (49 decreased, 165 increased) following acute exposure to smoldering red oak condensate, and 172 genes were differentially expressed (107 decreased, 65 increased) following repeated exposure to smoldering red oak condensate (Fig. 2A and B, Table S4). 62 genes were significantly differentially expressed and changed in the same direction across both exposure paradigms (12 decreased, 50 increased), representing a small proportion of the total gene expression changes, with the majority of gene expression changes unique to each exposure paradigm (Fig. 2C and D). The magnitude of change in gene expression was similar between the acute and repeated paradigms, and the two genes with the highest positive $\log_2$ fold changes (*TIPARP* and *CYP1B1*) were the same in both the acute and repeated exposure. Genes that were significantly increased in both exposure paradigms also included *SPDEF* and *IL24*, and genes that were significantly decreased in both exposure paradigms included *EDN2*, *IL33*, and *WNT10A*, demonstrating a small degree of consistency in molecular responses to red oak condensate over time. Genes that were uniquely increased following acute exposure included *IL19*, *TIMP3*, and *TNFRSF11A*, and genes that were uniquely decreased included *ADRA2A*, *EGR3*, and *NR2F2*. Genes that were uniquely increased in expression following repeated exposure included *NQO1*, *TGFBI*, and *KRT5*, and genes that were uniquely decreased included *PGF*,

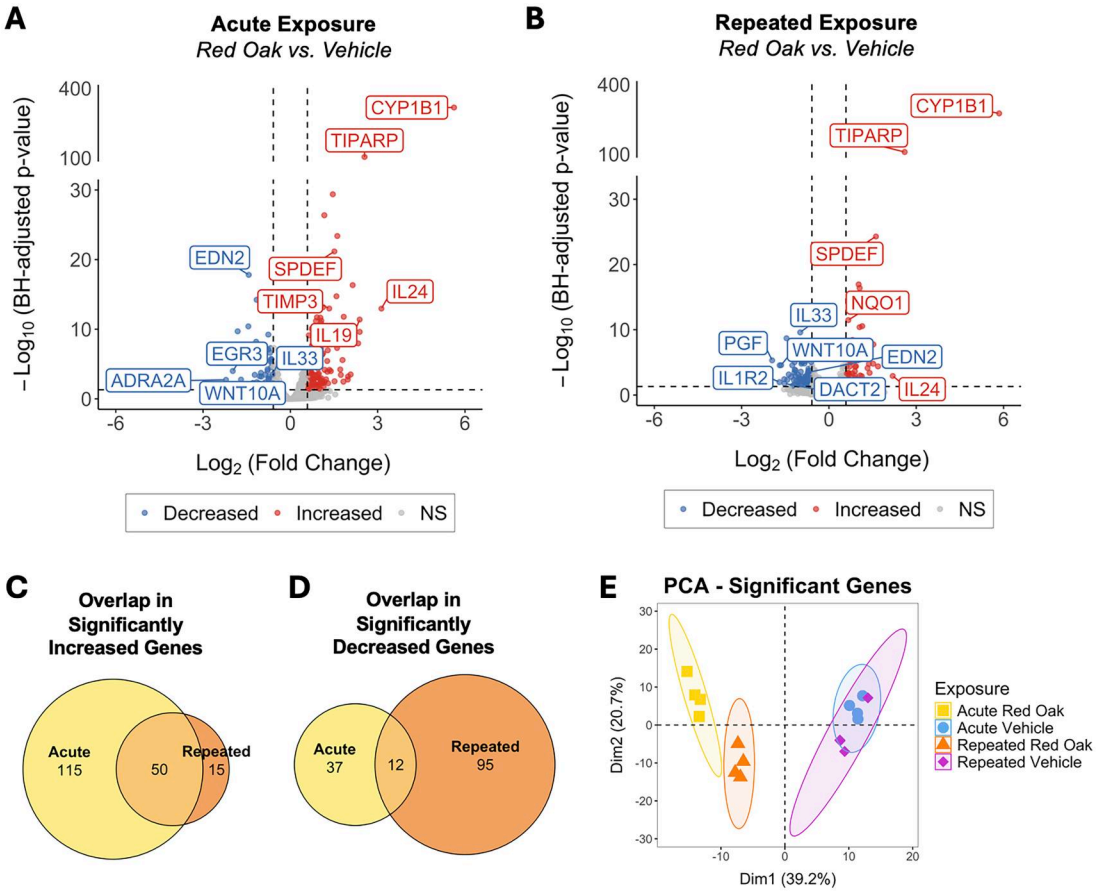

Fig. 2. RNAseq differential expression results for acute and repeated exposure to smoldering red oak condensate. (A, B) Volcano plots showing differential expression results, with genes with significantly increased expression highlighted in red and significantly decreased expression highlighted in blue. Genes highlighted were selected to provide examples of genes shared and unique to each exposure paradigm, genes with known roles in lung biology, and genes with high fold change and low *P*-values. Genes were considered significantly differentially expressed with adjusted *P*-value < 0.05 and $|\log_2$ fold change$| > 0.585$. (C, D) Euler plots of the overlap in significantly increased and decreased genes between the acute and repeated exposure paradigms. (E) Principal component analysis of significantly differentially expressed genes with exposure overlaid.

IL1R2, and *DACT2*. Notably, principal component analysis on significantly differentially expressed genes demonstrated clustering of acute and repeated red oak-exposed samples separately from each other and from the vehicle samples, whereas vehicle samples clustered together (Fig. 2E). This suggests minimal effects of repeated exposure to the vehicle control and confirms, in general, the overall unique gene expression profiles following acute and repeated exposure to smoldering red oak condensate.

RNA sequencing pathway analysis

Pathway analysis with significantly differentially expressed genes was used to further understand biological changes occurring with acute and repeated exposure to smoldering red oak condensate (Table 1). Following acute exposure, 8 pathways were predicted to be activated, and 1 pathway was predicted to be inhibited. Activated pathways were primarily related to cell signaling (S100 family signaling, IL-15 production, IL-10 signaling), stem cell biology, and pulmonary fibrosis, whereas the IL-27 signaling pathway was predicted to be inhibited. Genes that were associated with the greatest number of activated/inhibited pathways following acute exposure were *FGFR1* (n = 6 pathways), *SMAD3* (n = 6), *FGFRL1* (n = 4), *WNT10A* (n = 4), and *WNT9A* (n = 4). In contrast, 11 pathways were predicted to be inhibited following repeated exposure, including pathways related to fibrosis and cytokine signaling. Genes that were associated with the greatest number of pathways following repeated exposure were *TGFB2* (n = 6 pathways), *FZD8* (n = 5), *NGFR* (n = 5), and *WNT4* (n = 5). Similar to the differential expression results, the pathway analysis results demonstrate increases in molecular pathway signaling associated with acute exposure followed by decreases in signaling associated with repeated exposure. For full pathway analysis results, see Tables S5 and S6.

Secreted protein differential expression

To assess whether exposures resulted in changes in protein secretion, we measured the concentration of secreted proteins in the basolateral media before and after each day of exposure (days 1, 3, 5, 8, 10, and 12). Interestingly, PCA suggested that donor-specific differences in protein secretion were reduced following exposure, as indicated by greater overlap among donors (Fig. S3B and E). To statistically evaluate this observation, a multivariate dispersion test was conducted, which confirmed a significant difference in sample dispersion between the pre- and postexposure datasets (Table S7). To determine whether these differences persisted after accounting for donor-specific and temporal effects, we next applied a mixed-effects model incorporating donor and timepoint as random and fixed factors,

Table 1. Pathway analysis results.

Acute exposure		
Pathway	**Z-score**	**Genes in pathway**
S100 Family Signaling Pathway	2.524	*ADGRF1, ADRA2A, ADRB1, AREG, CDKN1A, CXCL8, DLC1, FGFR1, FGFRL1, GPR68, LPAR6, MAP3K8, PLAT, PTGER4, PTGFR, S100A2, SMAD3, WNT10A, WNT9A*
Pulmonary Fibrosis Idiopathic Signaling Pathway	2.309	*AJUBA, AREG, EGR1, FGFR1, FGFRL1, FOXO6, ITGA2, JARID2, SMAD3, THBS1, WNT10A, WNT9A*
Transport of inorganic cations/anions and amino acids/oligopeptides	2.236	*SLC20A1, SLC5A8, SLC6A6, SLC7A5, SLC8B1*
IL-15 Production	2.236	*ABL2, CLK3, CSK, DYRK3, FGFR1*
IL-10 Signaling	2.236	*CDKN1A, IL1RN, IL33, IL4R, PRDM1*
Transcriptional Regulatory Network in Embryonic Stem Cells	2.121	*FGFR1, FGFRL1, FOXC1, ISL1, KLF4, SMAD3, WNT10A, WNT9A*
Osteoarthritis Pathway	2.121	*CXCL8, FGFR1, ITGA2, NAMPT, PPARGC1A, PTGS2, SMAD3, SPHK1, TIMP3*
Human Embryonic Stem Cell Pluripotency	2.121	*FGFR1, FGFRL1, KLF4, SMAD3, SPHK1, TFCP2L1, WNT10A, WNT9A*
IL-27 Signaling Pathway	−2.236	*LPAR6, PPARGC1A, PTGS2, SMAD3, TLR5*
Repeated exposure		
Pathway	**Z-score**	**Genes in pathway**
Myelination Signaling Pathway	−2.111	*BMP2, DLC1, FGFRL1, FZD8, HES5, IRS1, LAMA3, NDRG1, NGFR, WNT10A, WNT4*
Role of Macrophages, Fibroblasts and Endothelial Cells in Rheumatoid Arthritis	−2.121	*DKK3, FZD8, IL1R2, IL32, IL33, NGFR, PGF, WNT10A, WNT4*
Elastic fiber formation	−2.236	*BMP2, ELN, LOX, LOXL4, TGFB2*
Hereditary Breast Cancer Signaling	−2.236	*GADD45A, GADD45B, PGF, TGFB2, UBD*
Factors Promoting Cardiogenesis in Vertebrates	−2.236	*BMP2, FZD8, TGFB2, WNT10A, WNT4*
Amyloid fiber formation	−2.449	*H2AC14, H2AC4, H2BC13, H2BC14, SNCA, TGFBI*
Hepatic Cholestasis	−2.449	*ABCB11, IL1R2, IL33, NGFR, TGFB2, TNFSF10*
TCF dependent signaling in response to WNT	−2.646	*CAV1, FZD8, H2AC14, H2BC13, H2BC14, SOX9, WNT4*
Chromatin Organization	−2.646	*H2AC14, H2BC13, H2BC14, H3C10, H3C12, H3C2, H3C8*
Pathogen Induced Cytokine Storm Signaling Pathway	−2.828	*COL17A1, CXCL2, HLA-DQB1, IL1R2, IL33, NGFR, PGF, SLC2A3, TGFB2, TNFSF10*
Hepatic Fibrosis Signaling Pathway	−2.828	*EDN1, FZD8, IL1R2, IL33, NGFR, PGF, TGFB2, WNT10A, WNT4*

Significantly differentially expressed genes ($|\log_2$ fold change$| > 0.585$, adjusted $P < 0.05$) were used as input for Ingenuity Pathway Analysis. Pathways with −log(BH adjusted P-value) >1.3 and z-scores >2 (predicted activated) or <2 (predicted inhibited) were included in the table.

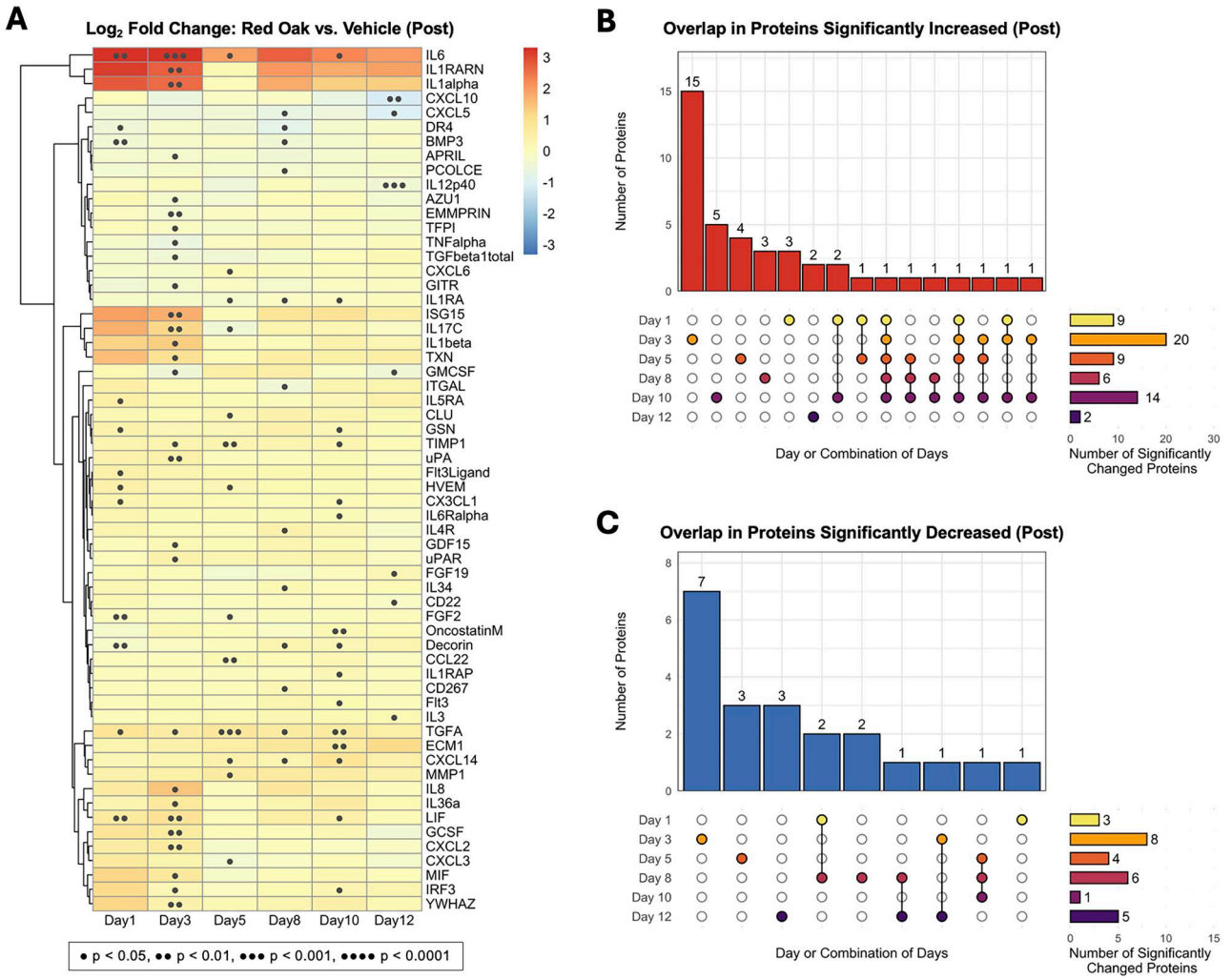

Fig. 3. Secreted proteins measured in post-exposure samples across days of the repeated exposure paradigm. (A) Heatmap showing average $\log_2$ fold change and statistical significance for proteins with a significant difference between red oak and vehicle on at least one of the days (n = 60 proteins). $\log_2$ fold change was calculated as red oak/vehicle control for each donor, then averaged and $\log_2$ transformed. Statistical significance was determined using paired *t*-tests. • $P < 0.05$, •• $P < 0.01$, ••• $P < 0.001$, and •••• $P < 0.0001$. Upset plots showing overlap in proteins (B) significantly increased or (C) significantly decreased across days of the repeated exposure. For example, the first bar of (B) shows that 15 proteins were uniquely significantly increased on day 3, and the seventh bar shows that 2 of the same proteins were significantly increased on days 1 and 10. The upset plots also show the total number of significantly increased and decreased proteins for each day on the horizontal bar chart next to the group matrix. For example, (B) shows that 9 proteins were significantly increased on day 1, 20 proteins were significantly increased on day 3, and 9 proteins were significantly increased on day 5.

respectively. This model confirmed that the observed reduction in dispersion persisted even after accounting for repeated measures (Table S8), suggesting that: (1) interindividual differences are more readily detected in the absence of toxicological insult, (2) responses to toxicological insult may have more commonalities across individuals, and/or (3) interindividual differences are more apparent for samples collected over longer periods of time (i.e., 48 to 72 h for accumulation of secreted proteins vs 4 h). For full statistical results across all detected proteins, alongside full protein names, see Tables S9 and S10.

In the post-exposure samples, there were 60 proteins with significantly different concentrations in conditioned media of red oak versus vehicle controls on at least one of the days (Fig. 3A), with a majority of these proteins significantly increased in red oak-exposed samples. On day 3, the day with the highest number of differentially secreted proteins, there were 28 proteins with significantly different concentrations (20 increased and 8 decreased), and most of these were unique to day 3 (Fig. 3B and C). Proteins with significantly increased concentrations across multiple days included IL6, TGFα, TIMP1, CXCL14, and LIF. By day 12, most significantly differentially secreted proteins were decreased in concentration. The proteins with the greatest decrease in concentration were CXCL10, CXCL5, and GMCSF. Only two differentially secreted proteins changed directionality across days: (i) IL17C was significantly increased on day 3 and significantly decreased on day 5; (ii) Decorin was significantly decreased on day 1 and significantly increased on days 5 and 8. Thus, the majority of significantly differentially secreted proteins were either increased or decreased in concentration across the repeat exposures demonstrating a degree of consistency across biological responses over time.

In the pre-exposure conditioned media samples, there were 75 proteins with significantly different concentrations between red oak and vehicle on at least one of the days (Fig. 4A). The days with the highest number of significantly differentially secreted proteins were day 5 (22 increased, 6 decreased) and day 12 (13 increased, 14 decreased) (Fig. 4B and C). Proteins with significantly increased concentrations across multiple days included CXCL14, MMP1, FLT3L, CCL22, CD46, and SCF. Paralleling the

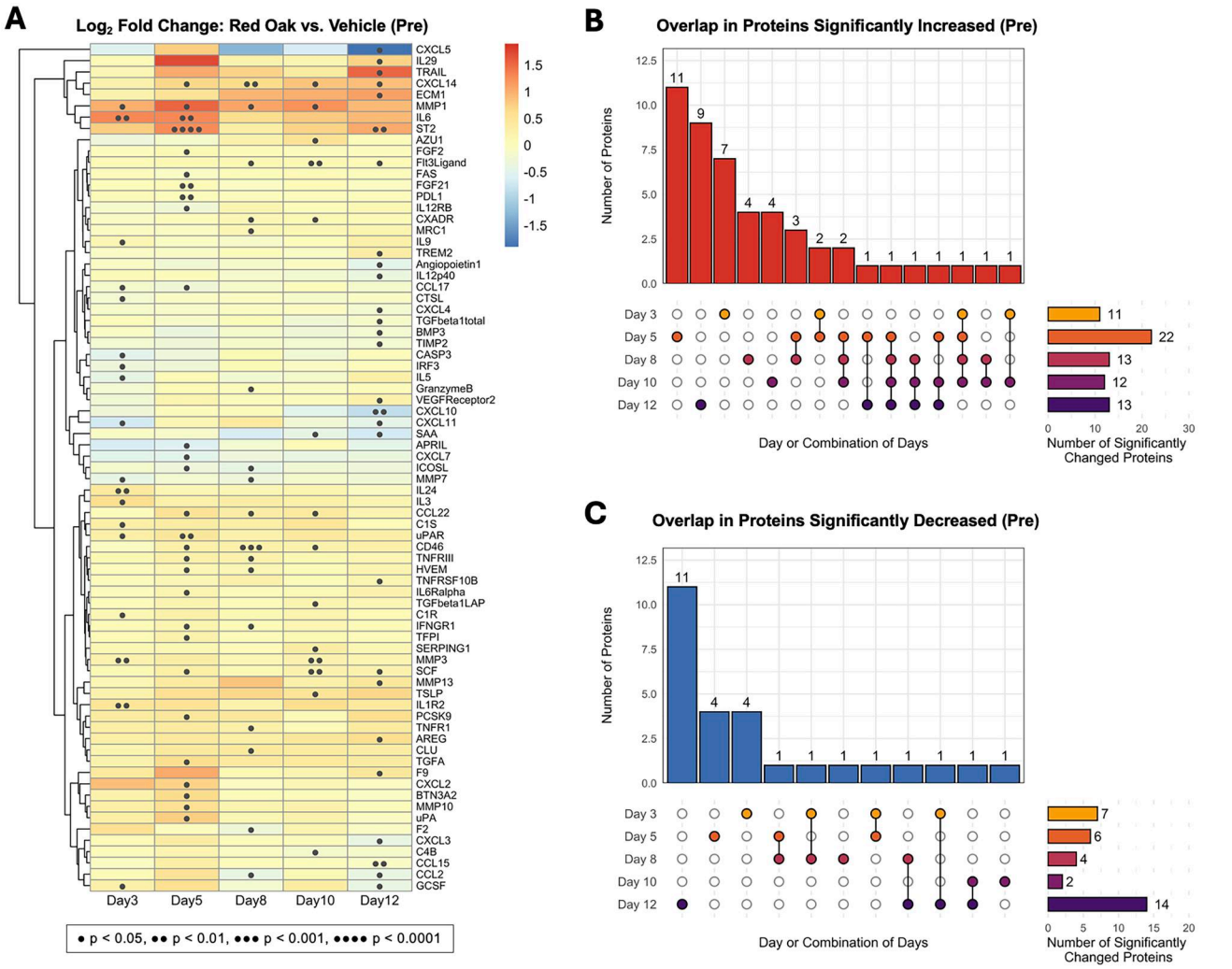

Fig. 4. Secreted proteins measured in pre-exposure samples across days of the repeated exposure paradigm. (A) Heatmap showing average log_2 fold change and statistical significance for proteins with a significant difference between red oak and vehicle on at least one of the days (n = 75 proteins). Log_2 fold change was calculated as red oak/vehicle control for each donor, then averaged and log_2 transformed. Statistical significance was determined using paired t-tests. • $P < 0.05$, •• $P < 0.01$, ••• $P < 0.001$, and •••• $P < 0.0001$. (B, C) Upset plots showing overlap in proteins significantly increased (B) or significantly decreased (C) across days of the repeated exposure and showing the total number of significantly increased and decreased proteins for each day. For example, the first bar of (B) shows that 11 proteins were uniquely significantly increased on day 5, and the fourth bar shows that 2 of the same proteins were significantly increased on days 5 and 8. The upset plots also show the total number of significantly increased and decreased proteins for each day on the horizontal bar chart next to the group matrix. For example, (B) shows that 7 proteins were significantly increased on day 3, and 6 proteins were significantly increased on day 5.

postexposure data, CXCL5 and CXCL10 were significantly decreased on day 12. Importantly, the pre-exposure data demonstrate that even after exposure was removed, the cells did not fully recover before application of the next exposure.

Relationship between secreted protein and RNA sequencing data

To assess the agreement between gene expression changes and secreted protein levels following acute or repeated red oak exposures, we next compared detection, correlation, and significant changes in expression levels across the datasets (Fig. 5A). Specifically, we compared secreted protein levels on days 1 and 3 to acute gene expression changes, and we compared secreted protein levels on day 12 to gene expression changes on day 12 of the repeated exposure. Although we found high overlap in detection between the gene expression and secreted protein data, gene counts and protein concentrations were generally not well-correlated, with around 11% to 30% of proteins with concentration that correlated to the RNA sequencing raw counts for each pair of protein-to-gene (i.e., gene that encodes the same protein match). When comparing significantly differentially expressed genes and proteins, approximately half of the differentially expressed proteins had log_2 fold changes in the same direction in the RNA sequencing data. On day 1, two proteins (LIF and BMP3) were significantly differentially expressed in both the secreted protein and RNA sequencing data (Fig. 5B and C), and on day 3, two proteins (IL-24 and uPA-R) were significantly differentially expressed in both the secreted protein and RNA sequencing data (Fig. 5D and E). We hypothesize that lack of correlation between secreted protein and RNA sequencing data may be due to a number of factors, including the differences in analyzed samples (i.e., cell samples for RNA and conditioned media for protein), collection timepoint being the same for RNA and protein samples, differing detection technologies, low number of samples, post-translational modifications, and secretory mechanisms/protein transport from cells to media. Still, the changes

A **Summary of Relationships Between RNAseq and Secreted Protein Data**

	Protein Expression Data		
	Day 1 Post	Day 3 Pre	Day 12 Post
Analysis Set Up			
RNA Seq Comparison Dataset	Day 1 Post (Acute)	Day 1 Post (Acute)	Day 12 Post (Repeated)
N Proteins in RNAseq Data	145/181	158/210	145/181
Spearman Correlation Analysis (RNAseq Counts vs. Log2 Protein Concentration)			
$\|R\| > 0.6$	33/145	47/158	34/145
$\|R\| > 0.6$ & $p < 0.05$	16/145	21/158	16/145
Comparison of Significance and Log2 Fold Change			
Significant Proteins Detected in RNAseq Data	10/12	16/18	1/7
Log2 Fold Change Same Direction	5/10	14/16	0/7
Log2 Fold Change Same Direction and RNAseq $p < 0.05$	**2/10**	4/16	0/7
Log2 Fold Change Same Direction and RNAseq $p_{adj} < 0.05$	0/10	**2/16**	0/7

Bolded cells plotted in B-E below

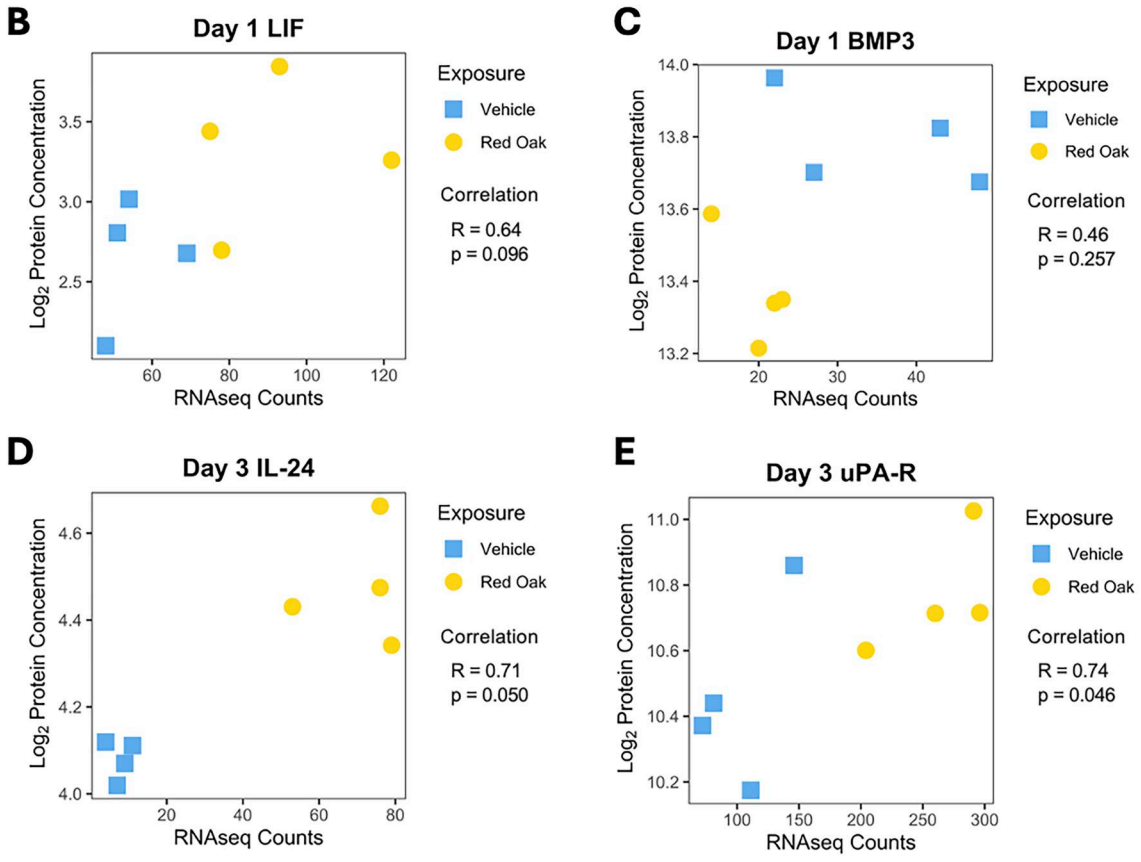

Fig. 5. Comparison of measurements and statistical significance between RNA sequencing and secreted protein data. (A) Table summarizing the approach and results for comparing RNA sequencing and secreted protein data. (B–E) Plots showing correlations between RNA sequencing raw counts and $\log_2$ protein concentrations for proteins with significant differences and shared directionality between groups (as bolded in part A).

that commonly persist across these differences in platforms, timepoints, and endpoints are worth highlighting.

Discussion

It is important to understand the effects of both acute and chronic exposures to WFS, as populations such as firefighters and community members are often repeatedly exposed to WFS. This study demonstrates the utility of differentiated primary HBECs for evaluating toxicological responses to WS over time, as we were able to implement single (4 h) and repeated (4 h/d, 3 d/wk, 2 wk) WS exposure while maintaining cell viability. Results indicate that transcriptional and secreted protein responses to WS are time-dependent, with increased markers of tissue

remodeling and immune response following acute exposure and decreased signaling following repeated exposure.

In both the acute and repeated exposure paradigm, genes with some of the highest positive $\log_2$ fold changes included *CYP1B*, which is involved in phase 1 metabolism of xenobiotics such as PAHs (Spivack et al. 2001); *TIPARP*, which inhibits hypoxia signaling (Zhang et al. 2020) and can promote angiogenesis (Miura et al. 2023); *IL24*, which has been hypothesized to play a role pulmonary fibrosis and wound healing (Rao et al. 2021); and *SPDEF*, which regulates goblet cell differentiation (Musthafa et al. 2023). Genes with some of the highest negative $\log_2$ fold changes included *IL33* and *WNT10A*. Increased *IL33* is associated with airway inflammation, asthma, and chronic obstructive pulmonary disease (COPD) (Calderon et al. 2023; Zhou et al. 2023), though lower expression has been also been observed in smokers (Faiz et al. 2023), and while increased *WNT10A* is associated with fibrosis (Oda et al. 2016; Chen et al. 2018), no studies to our knowledge have reported the biological implications of decreased *WNT10A* expression. These findings suggest some degree of consistency in response to acute versus repeated exposure to woodsmoke in pathways that have direct relevance to toxicant exposure and respiratory diseases.

However, despite these shared changes, the majority of significantly differentially expressed genes were unique to either the acute or repeated exposure samples. Following acute WS exposure, a higher number of genes were significantly increased in expression, including genes such as *IL19*, which is a pleiotropic cytokine involved in immune regulation and which is upregulated in lung fibrosis and asthma (Huang et al. 2008; Hoffman et al. 2011; Wang et al. 2022), and *TNFRSF1A*, which is increased in asthma and lung cancer. Interestingly, *TIMP3*, which exerts anti-inflammatory effects by breaking down metalloproteinases involved in inflammatory responses (Gill et al. 2013; Meunier et al. 2016), was also increased. Pathway analysis results paralleled individual gene results, with predicted activation of pathways relating to fibrosis and immune homeostasis. In contrast, following repeated exposure, more genes and pathways were significantly decreased/inhibited, including fibrosis-related pathways. It is possible that this phenomenon is due to negative feedback or adaptive mechanisms, wherein pathways are upregulated following acute exposure and then downregulated through negative feedback over time during the repeated exposure. For example, many heavy smokers do not develop lung cancer, which has been attributed to adaptation that may facilitate tolerance to toxic exposures (Huang et al. 2022). To further explore this hypothesis, additional studies examining pathway-specific responses in greater mechanistic depth are needed. It is also important to recognize that responses relating to wound healing and tissue repair, such as broad pathway activation in the acute exposure paradigm and upregulation of *TGFB* and *KRT5* in the chronic exposure paradigm, may represent either physiologic injury and repair processes or may contribute to pathological wound repair.

Both the acute and repeated exposure findings we report here are largely unique in comparison with previous in vitro and rodent in vivo studies characterizing the effects of WFS and WS, which have generally only focused on immune and inflammatory phenotypes (Sussan et al. 2014; Vose et al. 2021; Upadhyay et al. 2024; Heibati et al. 2025; Noël et al. 2025). We hypothesize that differences in findings between studies are due to differences in experimental models and exposure paradigms as well as differences in endpoints assessed, as previous studies focused on inflammatory cell infiltration and secretion of smaller sets of cytokines and chemokines. For example, many cell culture studies report an increase in IL-8 following acute WS condensate exposure, which we did not observe; however, these studies were all either conducted in cell lines or with longer exposure lengths (24 h) (Perng et al. 2013; Heibati et al. 2025), suggesting that some responses only occur with longer exposure windows than were used in our study. Notably, similar to previously published studies of nasal and central airway secreted protein responses in human participants following acute smoldering red oak exposure (Rebuli et al. 2019; Nalesnik et al. 2026) and a study of differentiated nasal epithelial cells exposed to smoldering red oak condensate (Brocke et al. 2022), we did not find a significant increase in secretion of proinflammatory proteins IL-8 or TNF-α. Importantly, our results demonstrate early changes in genes and pathways important in lung injury and repair. These pathways also play a role in pathogenic processes in multiple lung diseases, such as asthma, COPD, and pulmonary fibrosis. Thus, these data support previously reported associations between WFS/WS/PM exposure and lung disease development (Orr et al. 2020; Cui et al. 2023; Xing et al. 2025) and exacerbation (Delfino et al. 2009; Reid et al. 2016; Winterbottom et al. 2018). However, additional studies are needed to more specifically understand the sequence of events from initial perturbation to development, progression, and/or exacerbation of each specific lung disease.

To further explore temporal variation in response to WS exposure, we measured a panel of secreted proteins in basolateral media collected immediately following exposure on each day ("post") and prior to exposure on subsequent days of the repeated exposure ("pre"). We observed significant increases in many proinflammatory proteins, including IL-6, IL-1α, MMP1, and IL-8, on days 1 and 3, with this effect disappearing on days that were later in the repeated exposure. By day 12, a number of proteins were significantly decreased, most notably CXCL5 and CXCL10. CXCL5 has been shown to regulate recruitment of neutrophils and lymphocytes to the airway, with decreased CXCL5 resulting in increased B lymphocytes (Guo et al. 2021); thus, decreased CXCL5 following WS exposure could have implications for Th2-related disease processes and responses to respiratory infections. In contrast, increased CXCL10 has been associated with inflammation and disease severity, so the decrease in CXCL10 we observed may serve as a compensatory response following repeated inflammatory insult (Ding et al. 2025). Statistical findings also support an interesting temporal trend, wherein interindividual differences in secreted proteins become muted immediately after WFS exposures, and then re-appear after a few days of recovery, supporting the timing element of sample collection being critical in future in vitro studies.

Although this study represents an advancement toward understanding the toxicity and underlying cellular processes impacted by wildfire-relevant exposures in the lung, we recognize limitations that could be addressed in future investigations. For example, we used cells from four donors (two males and two females), which were sufficient for detecting differentially expressed genes and proteins but could be expanded to better assess interindividual variability, such as sex- and age-dependent differences in response to WS over time. Another source of interindividual variability in response to exposure could include epigenetic memory from previous exposures (Clark and Rager 2020), though previous environmental exposures would be difficult to evaluate from deceased donors. Aside from visual inspection, we also did not assess whether any condensate remained on the surface of the cultures or inside the cells after removing the exposure and washing the cells. If any condensate

remained on the surface or inside of the cells, our results could reflect the effects of sustained insult that may accumulate over time, and this type of exposure may also occur *in vivo* in lung. To better understand WS particle accumulation in lung cells, more studies are needed, particularly comparing in vitro versus in vivo models.

We also recognize that, given the high degree of variation in wildfire-relevant smoke emission chemistries (Kim et al. 2018; Koval et al. 2022), it will be important for future studies to incorporate more than one type of WFS-relevant exposure, to expose cells at ALI to whole smoke, and to include photochemically aged smoke condensates (Kim et al. 2023) to fully capture the range of potential chemical exposures that occur as a result of wildfires and to more accurately model repeated exposures, which are more likely to include photochemically aged smoke. It would also be valuable to compare diluting condensate in media versus PBS or another buffer solution, as there is potential for interaction between chemicals in the condensate with components of the cell culture media and potential for different responses of cells to apical PBS versus media treatment, even in the absence of chemical exposure. Future studies that include collection of a wider range of sample types at interim time points, determine how long it takes for cells to recover, repeat exposures over a longer period of time, and model continuous exposure will also provide needed insight into the temporal dynamics of response to WS exposure and better model a broad range of real-world WFS exposure scenarios. In addition to limitations relating to the experimental paradigm, our assessment of biological endpoints was limited to gene expression and protein concentration, which may not necessarily capture protein or signaling pathway activity. Finally, although differentiated primary human airway epithelial cell cultures include multiple cell types present in the airway epithelium in vivo, future studies using single-cell sequencing are needed to understand cell-specific responses in these cultures. Many of our findings were related to the adaptive immune system and fibrosis; therefore, advanced approaches that enable assessment of interactions between immune cells, fibroblasts, and epithelial cells, such as multilayered cell culture models, organoids, and organ-on-a-chip, are needed to expand upon these findings. Relatedly, in vitro cultures lack clearance mechanisms found in the lungs in vivo, such as mucociliary transport and macrophage phagocytosis, which can limit comparisons between in vitro exposure paradigms and real-world exposures in humans.

Overall, our findings demonstrate unique biological responses following acute versus repeated exposure to WS and provide a novel lens into the molecular mechanisms underlying WS exposure effects through unbiased assessment of the cellular transcriptome and secretome. These data also serve to inform future studies investigating temporal variation in response to acute and repeated WS exposure. Taken together, these findings support a growing body of literature on the respiratory effects of WFS exposure and highlight the importance of studying long-term exposure to WFS.

Acknowledgments

We thank Gabriela E. De la Cruz and Lily Wai in the Pathology Services Core for expert technical assistance with histopathology. The PSC is supported in part by an NCI Center Core Support Grant (P30CA016086). We thank Dr Phillip Clapp, Dr Charlotte Love, Dr Nicolas Mallek, and Sarah Lester for sharing protocols and advice related to growing primary human bronchial epithelial cells. This work used the Nomic high-throughput protein profiling platform from Nomic Bio (Montreal, Canada).

Supplementary material

Supplementary material is available at *Toxicological Sciences* online.

Funding

This study was supported by research grants from the National Institutes of Health (NIH) including the National Institute of Environmental Health Sciences (NIEHS) T32ES007126 (CC), T32ES007126 (JC), F32ES036096 (EH), and R01ES035878 (JR). Additional support was provided by the UNC Institute for Environmental Health Solutions (IEHS).

Conflicts of interest. The study authors declare no conflict of interest.

Data availability

Raw and processed RNA sequencing data are available via Gene Expression Omnibus under the accession GSE288818. Raw and processed multi-plex protein expression data and supplemental tables are available via the Ragerlab-Dataverse (Hickman et al. 2026). All associated input files and script are available via the Ragerlab GitHub (2026).

Disclaimer

The views expressed in this article are those of the author(s) and do not necessarily represent the views or the policies of the U.S. Environmental Protection Agency. Any mention of trade names, manufacturers or products does not imply an endorsement by the United States Government or the U.S. Environmental Protection Agency. EPA and its employees do not endorse any commercial products, services, or enterprises.

References

Alford KL, Kumar N. 2021. Pulmonary health effects of indoor volatile organic compounds – a meta-analysis. Int J Environ Res Public Health. 18:1578.

Barregard L, Sällsten G, Andersson L, Almstrand AC, Gustafson P, Andersson M, Olin AC. 2008. Experimental exposure to wood smoke: effects on airway inflammation and oxidative stress. Occup Environ Med. 65:319–324.

Bates D, Mächler M, Bolker B, Walker S. 2015. Fitting linear mixed-effects models using lme4. J Stat Soft. 67:1–48.

Bazina L, Deloid G, Fritzky L, Lizonova D, Vaze N, Demokritou P. 2025. Impact of Canadian wildfire-emitted particulate matter on THP-1 lung macrophage health and function. Environ Sci Technol. 59:3869–3883.

Black C, Tesfaigzi Y, Bassein JA, Miller LA. 2017. Wildfire smoke exposure and human health: significant gaps in research for a growing public health issue. Environ Toxicol Pharmacol. 55:186–195.

Braakhuis HM, He R, Vandebriel RJ, Gremmer ER, Zwart E, Vermeulen JP, Fokkens P, Boere J, Gosens I, Cassee FR. 2020. An air-liquid interface bronchial epithelial model for realistic, repeated inhalation exposure to airborne particles for toxicity testing. J Vis Exp. 2020:e61210. https://doi.org/10.3791/61210

Brocke SA, Billings GT, Taft-Benz S, Alexis NE, Heise MT, Jaspers I. 2022. Woodsmoke particle exposure prior to SARS-CoV-2 infection alters antiviral response gene expression in human nasal epithelial cells in a sex-dependent manner. Am J Physiol Lung Cell Mol Physiol. 322:L479–L494.

Buford M, Lacher S, Slattery M, Levings DC, Postma B, Holian A, Migliaccio C. 2024. A mouse model of wildfire smoke-induced health effects: sex differences in acute and sustained effects of inhalation exposures. Inhal Toxicol. 36:367–377.

Burbank AJ, Vadlamudi A, Mills KH, Alt EM, Wells H, Zhou H, Alexis N, Hernandez ML, Peden DB. 2019. The glutathione-s-transferase mu-1 null genotype increases wood smoke-induced airway inflammation. J Allergy Clin Immunol. 143:2299–2302.e3.

Calderon AA, Dimond C, Choy DF, Pappu R, Grimbaldeston MA, Mohan D, Chung KF. 2023. Targeting interleukin-33 and thymic stromal lymphopoietin pathways for novel pulmonary therapeutics in asthma and COPD. Eur Respir Rev. 32:220144.

Chen H, Samet JM, Bromberg PA, Tong H. 2021. Cardiovascular health impacts of wildfire smoke exposure. Part Fibre Toxicol. 18:2.

Chen X, Shi C, Cao H, Chen L, Hou J, Xiang Z, Hu K, Han X. 2018. The hedgehog and Wnt/β-catenin system machinery mediate myofibroblast differentiation of LR-MSCs in pulmonary fibrogenesis. Cell Death Dis. 9:639.

Clark J, Rager JE. 2020. Chapter 1 – epigenetics: an overview of CpG methylation, chromatin remodeling, and regulatory/noncoding RNAs. In: Fry RC, editor. Environmental epigenetics in toxicology and public health. Academic Press. p. 3–32.

Cochran SJ, Dunigan-Russell K, Hutton GM, Nguyen H, Schladweiler MC, Jones DP, Williams WC, Fisher AA, Gilmour MI, Dye JA, *et al.* 2024. Repeated exposure to eucalyptus wood smoke alters pulmonary gene and metabolic profiles in male long-evans rats. Toxicol Sci. 199:332–348.

Cui F, Sun Y, Xie J, Li D, Wu M, Song L, Hu Y, Tian Y. 2023. Air pollutants, genetic susceptibility and risk of incident idiopathic pulmonary fibrosis. Eur Respir J. 61:2200777.

Dagher M, Ongo G, Robichaud N, Kong J, Rho W, Teahulos I, Tavakoli A, Bovaird S, Merjaneh S, Tan A, *et al.* 2025. nELISA: a high-throughput, high-plex platform enables quantitative profiling of the inflammatory secretome. Nat Methods. 22:2375–2385.

de Lagarde VM, Chevalier L, Méausoone C, Cazier F, Dewaele D, Cazier-Dennin F, Janona M, Logie C, Achard S, André V, *et al.* 2024. Acute and repeated exposures of normal human bronchial epithelial (NHBE) cells culture to particles from a coloured pyrotechnic smoke. Environ Toxicol Pharmacol. 105:104327.

Delfino RJ, Brummel S, Wu J, Stern H, Ostro B, Lipsett M, Winer A, Street DH, Zhang L, Tjoa T, *et al.* 2009. The relationship of respiratory and cardiovascular hospital admissions to the southern California wildfires of 2003. Occup Environ Med. 66:189–197.

Dillon G, Menakis J, Fay F. 2015. Wildland fire potential: a tool for assessing wildfire risk and fuels management needs. In: Keane RE, Jolly M, Parsons R, Riley K, editors. Proceedings of the large wildland fires conference; May 19-23, 2014; Missoula, MT. Proc. RMRS-P-73. Fort Collins (CO): U.S. Department of Agriculture, Forest Service, Rocky Mountain Research Station. p. 60–76.

Ding W, Wang P, Ding Z, Yang B, Huo S, Lin P, Zhao J, Xu Y, Ding S. 2025. CXCL10 modulates airway inflammation in asthma via Sirt3-dependent macrophage homeostasis. Life Sci. 379:123849.

Durinck S, Moreau Y, Kasprzyk A, Davis S, De Moor B, Brazma A, Huber W. 2005. BioMart and Bioconductor: a powerful link between biological databases and microarray data analysis. Bioinformatics. 21:3439–3440.

Durinck S, Spellman PT, Birney E, Huber W. 2009. Mapping identifiers for the integration of genomic datasets with the R/Bioconductor package biomaRT. Nat Protoc. 4:1184–1191.

Faiz A, Mahbub RM, Boedijono FS, Tomassen MI, Kooistra W, Timens W, Nawijn M, Hansbro PM, Johansen MD, Pouwels SD, *et al.* 2023. IL-33 expression is lower in current smokers at both transcriptomic and protein levels. Am J Respir Crit Care Med. 208:1075–1087.

Firke S. 2024. Janitor: simple tools for examining and cleaning dirty data. R Package Version 2.2.1. https://cran.r-project.org/web/packages/janitor/index.html

Fulcher ML, Gabriel S, Burns KA, Yankaskas JR, Randell SH. 2005. Well-differentiated human airway epithelial cell cultures. Methods Mol Med. 107:183–206.

Fulcher ML, Randell SH. 2013. Human nasal and tracheo-bronchial respiratory epithelial cell culture. Methods Mol Biol. 945:109–121.

Ghio AJ, Soukup JM, Case M, Dailey LA, Richards J, Berntsen J, Devlin RB, Stone S, Rappold A. 2012. Exposure to wood smoke particles produces inflammation in healthy volunteers. Occup Environ Med. 69:170–175.

Gill SE, Gharib SA, Bench EM, Sussman SW, Wang RT, Rims C, Birkland TP, Wang Y, Manicone AM, McGuire JK, *et al.* 2013. Tissue inhibitor of metalloproteinases-3 moderates the proinflammatory status of macrophages. Am J Respir Cell Mol Biol. 49:768–777.

Guo L, Li N, Yang Z, Li H, Zheng H, Yang J, Chen Y, Zhao X, Mei J, Shi H, *et al.* 2021. Role of CXCL5 in regulating chemotaxis of innate and adaptive leukocytes in infected lungs upon pulmonary influenza infection. Front Immunol. 12:785457.

Hansson A, Rankin G, Uski O, Friberg M, Pourazar J, Lindgren R, García-López N, Boman C, Sandström T, Behndig A, *et al.* 2023. Reduced bronchoalveolar macrophage phagocytosis and cytotoxic effects after controlled short-term exposure to wood smoke in healthy humans. Part Fibre Toxicol. 20:30.

Hao H, Xu K, Zhang D, Deng Y, Al-Kindi S, Pattisapu VK, Steenland K, Chang HH, Alonso A, Liu Y. 2025. Long-term wildfire smoke exposure and increased risk of heart failure in older adults. J Am Coll Cardiol. 85:2439–2451.

Hargrove MM, Kim YH, King C, Wood CE, Gilmour MI, Dye JA, Gavett SH. 2019. Smoldering and flaming biomass wood smoke inhibit respiratory responses in mice. Inhal Toxicol. 31:236–247.

Heibati B, Renz H, Lacy P. 2025. Wildfire and wood smoke effects on human airway epithelial cells: a scoping review. Environ Res. 272:121153.

Hickman E, Chou C, Seifert C, Chappel J, Kim YH, Corteselli E, Rager JE. 2026. Dataset for temporal variation in markers of immune signaling and wound repair in primary human airway epithelial cells following acute vs. repeated woodsmoke condensate exposure. V1 ed. UNC Dataverse. https://doi.org/10.15139/s3/ypitye

Hoffman C, Park SH, Daley E, Emson C, Louten J, Sisco M, de Waal Malefyt R, Grunig G. 2011. Interleukin-19: a constituent of the regulome that controls antigen presenting cells in the lungs and airway responses to microbial products. PLoS One. 6:e27629.

Huang F, Wachi S, Thai P, Loukoianov A, Tan KH, Forteza RM, Wu R. 2008. Potentiation of IL-19 expression in airway epithelia by IL-17a and IL-4/IL-13: important implications in asthma. J Allergy Clin Immunol. 121:1415–1421. 1421.e1411-1413.

Huang Z, Sun S, Lee M, Maslov AY, Shi M, Waldman S, Marsh A, Siddiqui T, Dong X, Peter Y, *et al.* 2022. Single-cell analysis of somatic mutations in human bronchial epithelial cells in relation to aging and smoking. Nat Genet. 54:492–498.

Hurteau MD, Westerling AL, Wiedinmyer C, Bryant BP. 2014. Projected effects of climate and development on California wildfire emissions through 2100. Environ Sci Technol. 48:2298–2304.

Janbazacyabar H, van Bergenhenegouwen J, Varasteh S, Garssen J, Folkerts G, Braber S. 2022. Repeated exposure of bronchial epithelial cells to particular matter increases allergen-induced cytokine release and permeability. Cytokine. 154:155878.

Kassambara A. 2023. Rstatix: pipe-friendly framework for basic statistical tests. R Package Version 0.7.2. https://cran.r-project.org/web/packages/rstatix/index.html

Kassambara A. 2025. Ggpubr: 'Ggplot2' based publication ready plots. R Package Version 0.6.1. https://cran.r-project.org/web/packages/ggpubr/index.html

Kassambara A, Mundt F. 2020. Factoextra: extract and visualize the results of multivariate data analyses. R Package Version 1.0.7. https://cran.r-project.org/web/packages/factoextra/index.html

Kim YH, Sinha A, George IJ, DeMarini DM, Grieshop AP, Gilmour MI. 2023. Toxicity of fresh and aged anthropogenic smoke particles emitted from different burning conditions. Sci Total Environ. 892:164778.

Kim YH, Warren SH, Krantz QT, King C, Jaskot R, Preston WT, George BJ, Hays MD, Landis MS, Higuchi M, *et al.* 2018. Mutagenicity and lung toxicity of smoldering vs. flaming emissions from various biomass fuels: implications for health effects from wildland fires. Environ Health Perspect. 126:017011.

Kolde R. 2025. Pheatmap: pretty heatmaps. R Package Version 1.0.13. https://cran.r-project.org/web/packages/pheatmap/index.html

Korsiak J, Pinault L, Christidis T, Burnett RT, Abrahamowicz M, Weichenthal S. 2022. Long-term exposure to wildfires and cancer incidence in Canada: a population-based observational cohort study. Lancet Planet Health. 6:e400–e409.

Koval LE, Carberry CK, Kim YH, McDermott E, Hartwell H, Jaspers I, Gilmour MI, Rager JE. 2022. Wildfire variable toxicity: identifying biomass smoke exposure groupings through transcriptomic similarity scoring. Environ Sci Technol. 56:17131–17142.

Krassowski M. 2020. Complexupset. R Package Version 1.3.6. https://cran.r-project.org/web/packages/ComplexUpset/index.html

Kyung SY, Jeong SH. 2020. Particulate-matter related respiratory diseases. Tuberc Respir Dis (Seoul). 83:116–121.

Låg M, Øvrevik J, Refsnes M, Holme JA. 2020. Potential role of polycyclic aromatic hydrocarbons in air pollution-induced non-malignant respiratory diseases. Respir Res. 21:299.

Larsson J. 2024. Eulerr: area-proportional euler and venn diagrams with ellipses. R Package Version 7.0.2. https://cran.r-project.org/web/packages/eulerr/index.html

Lee W, Lee S, Yoon J-K, Lee D, Kim Y, Han YB, Kim R, Moon S, Park YJ, Park K, *et al.* 2023. A single-cell atlas of in vitro multiculture systems uncovers the in vivo lineage trajectory and cell state in the human lung. Exp Mol Med. 55:1831–1842.

Lex A, Gehlenborg N, Strobelt H, Vuillemot R, Pfister H. 2014. Upset: visualization of intersecting sets. IEEE Trans Vis Comput Graph. 20:1983–1992.

Liu D, Tager IB, Balmes JR, Harrison RJ. 1992. The effect of smoke inhalation on lung function and airway responsiveness in wildland fire fighters. Am Rev Respir Dis. 146:1469–1473.

Love MI, Huber W, Anders S. 2014. Moderated estimation of fold change and dispersion for RNA-seq data with DESeq2. Genome Biol. 15:550.

Mallek NM, McCullough SD. 2021. Measurement of trans-epithelial electrical resistance with EVOM2 and EndOhm cup. Research Square. https://doi.org/10.21203/rs.3.pex-1672/v1

Mancarci O. 2025. Genesynonym: quick access to gene synonym information. R Package Version 1.7.25.6.15, commit 3024349f0355e904e4e56dd8e676316fd9a60d61. 2025. https://github.com/oganm/geneSynonym

Mastalerz M, Dick E, Chakraborty A, Hennen E, Schamberger AC, Schröppel A, Lindner M, Hatz R, Behr J, Hilgendorff A, *et al.* 2022. Validation of in vitro models for smoke exposure of primary human bronchial epithelial cells. Am J Physiol Lung Cell Mol Physiol. 322:L129–L148.

Meunier I, Bocquet B, Labesse G, Zeitz C, Defoort-Dhellemmes S, Lacroux A, Mauget-Faysse M, Drumare I, Gamez A-S, Mathieu C, *et al.* 2016. A new autosomal dominant eye and lung syndrome linked to mutations in *TIMP3* gene. Sci Rep. 6:32544.

Migliaccio CT, Kobos E, King QO, Porter V, Jessop F, Ward T. 2013. Adverse effects of wood smoke PM(2.5) exposure on macrophage functions. Inhal Toxicol. 25:67–76.

Mirabelli MC, Künzli N, Avol E, Gilliland FD, Gauderman WJ, McConnell R, Peters JM. 2009. Respiratory symptoms following wildfire smoke exposure: airway size as a susceptibility factor. Epidemiology. 20:451–459.

Miura K, Koyanagi-Aoi M, Maniwa Y, Aoi T. 2023. Chorioallantoic membrane assay revealed the role of TIPARP (2,3,7,8-tetrachlorodibenzo-p-dioxin-inducible poly (ADP-ribose) polymerase) in lung adenocarcinoma-induced angiogenesis. Cancer Cell Int. 23:34.

Musthafa A, Ryanto GRT, Suraya R, Nagano T, Suzuki Y, Hara T, Hirata KI, Emoto N. 2023. Acute amelioration of inflammatory activity caused by endothelin-2 deficiency during acute lung injury. Kobe J Med Sci. 69:e96–e105.

Nalesnik M, Hickman E, Almond M, Herring L, Mordant AL, Mills AC, Payton A, Rager JE, Peden DB, Jaspers I, *et al.* 2026. Exploratory analysis of the impact of sex on sputum proteomic response to inhaled wood smoke in humans. Toxicol Sci. 209:kfaf150.

National Interagency Fire Center. 2025. National interagency standards for resource mobilization. Boise (ID): National Interagency Fire Center.

Navarro KM, Butler CR, Fent K, Toennis C, Sammons D, Ramirez-Cardenas A, Clark KA, Byrne DC, Graydon PS, Hale CR, *et al.* 2022. The Wildland Firefighter Exposure and Health Effect (WFFEHE) study: rationale, design, and methods of a repeated-measures study. Ann Work Expo Health. 66:714–727.

Noël A, Glenn CK, El Hajj O, Anosike A, Kumar K, Abdurrahman MI, Flanagan S, Callaham MA, Loudermilk EL, Roberts ET, *et al.* 2025. Differential in vitro lung cell toxicity of fresh and photochemically aged smoke aerosol emissions from simulated wildland fires of duff and surface fuels. ACS EST Air. 2:2251–2262.

Oda K, Yatera K, Izumi H, Ishimoto H, Yamada S, Nakao H, Hanaka T, Ogoshi T, Noguchi S, Mukae H. 2016. Profibrotic role of WNT10A via TGF-β signaling in idiopathic pulmonary fibrosis. Respir Res. 17:39.

Oksanen J, Simpson G, Blanchet F, Kindt R, Legendre P, Minchin P, O'Hara R, Solymos P, Stevens M, Szoecs E, *et al.* 2025. Vegan: community ecology package. R Package Version 2.8-0. https://cran.r-project.org/web/packages/vegan/index.html

Orr A, A L Migliaccio C, Buford M, Ballou S, Migliaccio CT. 2020. Sustained effects on lung function in community members following exposure to hazardous PM(2.5) levels from wildfire smoke. Toxics. 8:53.

Pedersen TL. 2025. Patchwork: the composer of plots. R Package Version 1.3.1. https://cran.r-project.org/web/packages/patchwork/index.html

Perng D-W, Chang T-M, Wang J-Y, Lee C-C, Lu S-H, Shyue S-K, Lee T-S, Kou YR. 2013. Inflammatory role of AMP-activated protein kinase signaling in an experimental model of toxic smoke inhalation injury. Crit Care Med. 41:120–132.

Peters B, Ballmann C, Quindry T, Zehner EG, McCroskey J, Ferguson M, Ward T, Dumke C, Quindry JC. 2018. Experimental woodsmoke exposure during exercise and blood oxidative stress. J Occup Environ Med. 60:1073–1081.

QIAGEN. 2025. Ingenuity Pathway Analysis (IPA) knowledgebase: canonical pathways for a dataset. Redwood City (CA): QIAGEN. [accessed August 12, 2025]. https://qiagen.my.salesforce-sites.com/KnowledgeBase/KnowledgeNavigatorPage? id=kA41i000000L5pACAS

R Core Team. 2025. R: a language and environment for statistical computing. Version 4.5.0. Vienna, Austria: R Foundation for Statistical Computing.

Ragerlab GitHub. 2026. https://github.Com/ragerlab

Ramirez-Moral I, Schuurman AR, van Linge CCA, Butler JM, Yu X, de Haan K, van Leeuwen S, de Vos AF, de Jong MD, Vieira Braga FA, *et al.* 2024. Single-cell transcriptomics reveals subset-specific metabolic profiles underpinning the bronchial epithelial response to flagellin. iScience. 27:110662.

Rao L-Z, Wang Y, Zhang L, Wu G, Zhang L, Wang F-X, Chen L-M, Sun F, Jia S, Zhang S, *et al.* 2021. IL-24 deficiency protects mice against bleomycin-induced pulmonary fibrosis by repressing IL-4-induced M2 program in macrophages. Cell Death Differ. 28:1270–1283.

Ravindra NG, Alfajaro MM, Gasque V, Huston NC, Wan H, Szigeti-Buck K, Yasumoto Y, Greaney AM, Habet V, Chow RD, *et al.* 2021. Single-cell longitudinal analysis of SARS-CoV-2 infection in human airway epithelium identifies target cells, alterations in gene expression, and cell state changes. PLoS Biol. 19:e3001143.

Rebuli ME, Speen AM, Martin EM, Addo KA, Pawlak EA, Glista-Baker E, Robinette C, Zhou H, Noah TL, Jaspers I. 2019. Wood smoke exposure alters human inflammatory responses to viral infection in a sex-specific manner. a randomized, placebo-controlled study. Am J Respir Crit Care Med. 199:996–1007.

Reid CE, Brauer M, Johnston FH, Jerrett M, Balmes JR, Elliott CT. CT. 2016. Critical review of health impacts of wildfire smoke exposure. Environ Health Perspect. 124:1334–1343.

Rein G, Huang X. 2021. Smouldering wildfires in peatlands, forests and the arctic: challenges and perspectives. Curr Opin Environ Sci Health. 24:100296.

Reisen F, Duran SM, Flannigan M, Elliott C, Rideout K. 2015. Wildfire smoke and public health risk. International Journal of Wildland Fire. 24:1029–1044.

Rice RB, Boaggio K, Olson NE, Foley KM, Weaver CP, Sacks JD, McDow SR, Holder AL, LeDuc SD. 2023. Wildfires increase concentrations of hazardous air pollutants in downwind communities. Environ Sci Technol. 57:21235–21248.

Risso D, Ngai J, Speed TP, Dudoit S. 2014. Normalization of RNA-seq data using factor analysis of control genes or samples. Nat Biotechnol. 32:896–902.

Rizzo LV, Rizzo M. 2025. Wildfire smoke and health impacts: a narrative review. J Pediatr (Rio J). 101:S56–S64.

Sacks JD, Migliaccio CT, Reid CE, Montrose L. 2025. Shifting the conversation on wildland fire smoke exposures: more smoke within and across years requires a new approach to inform public health action. ACS EST Air. 2:122–129.

Schauberger P, Walker A. 2025. openxlsx: read, write and edit xlsx files. R Package Version 4.2.8. https://cran.r-project.org/web/packages/openxlsx/index.html

Schollaert C, Connolly R, Cushing L, Jerrett M, Liu T, Marlier M. 2025. Air quality impacts of the January 2025 Los Angeles wildfires: insights from public data sources. Environ Sci Technol Lett. 12:911–917.

Schwartz C, Bølling AK, Carlsten C. 2020. Controlled human exposures to wood smoke: a synthesis of the evidence. Part Fibre Toxicol. 17:49.

Spivack SD, Hurteau GJ, Reilly AA, Aldous KM, Ding X, Kaminsky LS. 2001. CYP1B1 expression in human lung. Drug Metab Dispos. 29:916–922.

Sussan TE, Ingole V, Kim JH, McCormick S, Negherbon J, Fallica J, Akulian J, Yarmus L, Feller-Kopman D, Wills-Karp M, *et al.* 2014. Source of biomass cooking fuel determines pulmonary response to household air pollution. Am J Respir Cell Mol Biol. 50:538–548.

United States Forest Service. 2023. Whp2023 classified map. Missoula (MT): Missoula Fire Sciences Laboratory. https://research.Fs.Usda.Gov/firelab/understory/whp2023-classified-map

Upadhyay S, Chakraborty A, Thimraj TA, Baldi M, Steneholm A, Ganguly K, Gerde P, Ernstgård L, Palmberg L. 2022. Establishment of repeated in vitro exposure system for evaluating pulmonary toxicity of representative criteria air pollutants using advanced bronchial mucosa models. Toxics. 10:277.

Upadhyay S, Rahman M, Rinaldi S, Koelmel J, Lin EZ, Mahesh PA, Beckers J, Johanson G, Pollitt KJG, Palmberg L, *et al.* 2024. Assessment of wood smoke induced pulmonary toxicity in normal- and chronic bronchitis-like bronchial and alveolar lung mucosa models at air–liquid interface. Respir Res. 25:49.

Vitucci ECM, Carberry CK, Payton A, Herring LE, Mordant AL, Kim YH, Gilmour MI, McCullough SD, Rager JE. 2025. Wildfire-relevant woodsmoke and extracellular vesicles (EVS): alterations in EV proteomic signatures involved in extracellular matrix degradation and tissue injury in airway organotypic models. Environ Res. 264:120395.

VoPham T, Liu T, Cortez M, Karasaki S, Falkenberg NF, Zewdie HY, Lin J, Nondin C, Chao SLS, Knowlton T, *et al.* 2025. Exposure to outdoor air pollution, wildfires, and cancer survival in the United States. Cancer Epidemiol. 98:102899.

Vose A, McCravy M, Birukova A, Yang Z, Hollingsworth JW, Que LG, Tighe RM. 2021. Wood smoke particle exposure in mice reduces the severity of influenza infection. Toxicol Appl Pharmacol. 426:115645.

Wang Y, Sun S, Wang K, Zhang M, Li M, Zan Y, Huang Q, Wu S, Zhao W, Xu W, *et al.* 2022. Interleukin-19 aggravates pulmonary fibrosis via activating fibroblast through TGF-β/smad pathway. Mediators Inflamm. 2022:6755407.

Wei R, Wang J, Jia E, Chen T, Ni Y, Jia W. 2018. GSimp: a Gibbs sampler based left-censored missing value imputation approach for metabolomics studies. PLoS Comput Biol. 14:e1005973.

Wentworth GR, Aklilu YA, Landis MS, Hsu YM. 2018. Impacts of a large boreal wildfire on ground level atmospheric concentrations of PAHs, VOCs and ozone. Atmos Environ (1994). 178:19–30.

Westerling AL, Hidalgo HG, Cayan DR, Swetnam TW. 2006. Warming and earlier spring increase Western U.S. forest wildfire activity. Science. 313:940–943.

Wickham H, Averick M, Bryan J, Chang W, McGowan L, François R, Grolemund G, Hayes A, Henry L, Hester J, *et al.* 2019. Welcome to the tidyverse. J Open Source Softw. 4:1686.

Winterbottom CJ, Shah RJ, Patterson KC, Kreider ME, Panettieri RA, Rivera-Lebron B, Miller WT, Litzky LA, Penning TM, Heinlen K, *et al.* 2018. Exposure to ambient particulate matter is associated with accelerated functional decline in idiopathic pulmonary fibrosis. Chest. 153:1221–1228.

Xing M, Cui F, Zheng L, Ma Y, Wang J, Tang L, Chen N, Zhao X, Tian Y, Su B. 2025. Association of fine particulate matter constituents with chronic obstructive pulmonary disease and the effect modification of genetic susceptibility. Npj Clim Atmos Sci. 8:89.

Zavala J, Freedman AN, Szilagyi JT, Jaspers I, Wambaugh JF, Higuchi M, Rager JE. 2020. New approach methods to evaluate health risks of air pollutants: critical design considerations for in vitro exposure testing. Int J Environ Res Public Health. 17:2124.

Zhang L, Cao J, Dong L, Lin H. 2020. TiPARP forms nuclear condensates to degrade HIF-1α and suppress tumorigenesis. Proc Natl Acad Sci USA. 117:13447–13456.

Zhang Q, Wang Y, Xiao Q, Geng G, Davis SJ, Liu X, Yang J, Liu J, Huang W, He C, *et al.* 2025a. Long-range PM2.5 pollution and health impacts from the 2023 Canadian wildfires. Nature. 645:672–678.

Zhang Y, Xu R, Huang W, Ye T, Yu P, Yu W, Wu Y, Liu Y, Yang Z, Wen B, *et al.* 2025b. Respiratory risks from wildfire-specific PM2.5 across multiple countries and territories. Nat Sustain. 8:474–484.

Zhou Y, Xu Z, Liu Z. 2023. Role of IL-33-ST2 pathway in regulating inflammation: current evidence and future perspectives. J Transl Med. 21:902.

Zimmermann EJ, Das A, Huber A, Gawlitta N, Kuhn E, Schlager C, Gutmann B, Krebs T, Schnelle-Kreis J, Delaval MN, *et al.* 2025. Toxicological effects of long-term continuous exposure to ambient air on human bronchial epithelial Calu-3 cells exposed at the air-liquid interface. Environ Res. 269:120759.

Toxicological Sciences, 2026, 209, 1–16
https://doi.org/10.1093/toxsci/kfag035
Research Article